Landau-Levich dynamical menisci

By Maleki M.[1,2], **Reyssat M.**[2], **Duclaux V.**[3], **Quéré D.**[2], **Clanet C.**[3]

[1] Institute for Advanced Studies in Basic Sciences (IASBS), Zanjan 45195, P. O. Box 45195-1159, Iran [2] Physique et Mécanique des Milieux hétérogènes, UMR 7636 du CNRS, ESPCI, 75005 Paris, France. [3] IRPHE, UMR 6594, 49 rue F. Joliot-Curie, BP 146, 13384 Marseille, France

In the limit of small capillary number ($Ca \equiv \eta V_0/\gamma \ll 1$), the dynamical meniscus observed when a solid is removed at constant velocity (V_0) from a bath of wetting liquid (viscosity η, surface tension γ) is "stretched" : the film thickness along the wall decreases monotonously from the classical static meniscus region to entrained film. If the motion of the coated solid is reversed (it enters the bath instead of leaving it), the whole meniscus shape changes: then it buckles and presents a stationary wavy shape. Here we study and discuss both these situations.

---

1. Introduction

When a solid plate contacts a bath of wetting liquid, a meniscus forms close to the place where solid, liquid and air meet. Surface tension (denoted as γ) is responsible for this deformation of the bath, while gravity (we denote ρ as the liquid density) opposes it, so that the size of the meniscus is of the order of the so-called capillary length $\kappa^{-1} \equiv \sqrt{\gamma/\rho g}$, that is a few millimetres for most liquids. If the plate is moved at a velocity V_0, the meniscus is deformed, and the deformation depends on the direction of the motion.

If the plate is extracted from the bath, some liquid is entrained, and thus the meniscus is stretched. While its bottom part remains insensitive to the plate motion, a dynamic region sets at the top of the static meniscus, matching it with the entrained film. The characteristics of this dynamic meniscus were found to be crucial by Landau and Levich (1942) and Derjaguin (1943), since they impose the thickness of the film drawn by the solid plate. This thickness is the key parameter in many industrial processes (such as fiber coating, deposition of films on ophthalmic glasses, dip coating, etc.) [Ruschak (1985)], which explains why it was extensively studied in various geometries (tube, fiber, Hele-Shaw cells, etc.) [Bretherton (1961), Quéré (1999), Park and Homsy (1984)].

Conversely, plunging the dry plate inside the liquid also deforms the meniscus, which is observed to make a liquid wedge, meeting the solid with a non-zero angle. This angle increases with the immersion velocity, as early described by Hoffman (1975), Tanner (1979) or de Gennes (1985). The deformation in this case also raises an important practical question, in particular in the limit of high velocities, where the dynamic angle becomes of the order of 180°, leading to air entrainment [Eggers (2004)].

For both motions, the deformation is induced by viscous forces (which generally dominate inertia in the confined region of the meniscus tip), and resisted by surface tension. Hence, the capillary number, Ca, which compares both these forces is the key dynamic parameter to understand the meniscus deformation. It can be written $Ca \equiv \eta V_0/\gamma$, denoting η as the liquid viscosity. In the limit of small capillary numbers (studied in this
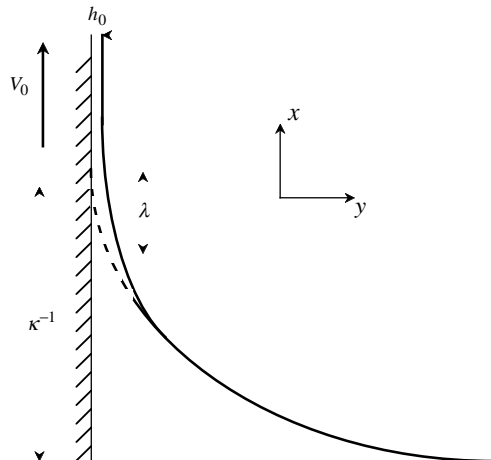
FIGURE 1. Sketch of the deformation of a liquid close to a moving plate. Owing to the motion, a dynamic meniscus (of length λ) forms at the top of the static meniscus (whose size if of the order of the capillary length κ^{-1}), and a film (of thickness h_0) is entrained by the plate.

paper), we expect the deformations to be modest, compared to the natural millimetric scale of the meniscus, κ^{-1}, implying need for special optical techniques to investigate the amplitude and nature of the deformations. Here we use an original experiment of reflectometry, and first describe the shape and characteristic dimension of the dynamic "stretched" meniscus, as entraining the plate. Then, we consider the reverse motion of a coated plate entering a bath, and show that "compression waves" then appear, contrasting with the more usual case of a dry solid, where a liquid wedge is observed. We describe the peculiarities of this wavy meniscus, and try to understand its physical origin.

2. Dragging a plate out of a wetting liquid

Figure 1 shows the deformation of the meniscus in the entrainment experiment. As a film (of thickness h_0) coats the plate, a dynamic meniscus (of characteristic length λ) sets at the top of the static meniscus. The curvature of this zone generates a depression below the surface, whose action is to suck the liquid entrained by viscosity along the plate. Since the slope of the profile is small, the Laplace pressure can be simply expressed as $-\gamma d^2h/dx^2$ (where h is the local thickness, and x the motion axis), so that the corresponding force per unit volume is: $\gamma d^3h/dx^3$. As early proposed by Landau and Levich (1942), in the limit of small capillary numbers ($Ca_0 \equiv \eta V_0/\gamma \ll 1$), gravity can be neglected in the description of the flow and the Navier-Stokes equation in the dynamic meniscus region reduces to: $\eta d^2u/dy^2 = -\gamma d^3h/dx^3$, where y is the direction perpendicular to the unidirectional flow u, along which velocity gradients take place.

Integrating this equation together with classical boundary conditions [no slip at the solid surface ($y = 0$), negligible viscous stress at the free surface ($y = h$)], a Poiseuille profile is found for the flow: $u(y) = V_0 - \gamma/2\eta d^3h/dx^3y(y - 2h)$. Integrating $u(y)$ over the film thickness, gives the flux of liquid. This quantity must be conserved, in particular in the region of the film where it writes h_0V_0, from which the differential equation of the film

profile $h(x)$ is deduced:

$$h_0 V_0 = h V_0 + \frac{\gamma}{3\eta} \frac{d^3 h}{dx^3} h^3 \tag{2.1}$$

As noted by Landau and Levich (1942), this equation can be made dimensionless by scaling the film thickness h by the quantity h_0, and the x variable by the length $\lambda \equiv h_0/(3Ca_0)^{1/3}$. Denoting these dimensionless lengths as $H = h/h_0$ and $X = x/\lambda$, equation (2.1) can be rewritten as:

$$\frac{d^3 H}{dX^3} = \frac{1-H}{H^3} \tag{2.2}$$

To satisfy the boundary condition $H(X = +\infty) = 1$ we can write, close to the film, $H(X) = 1 + \epsilon(X)$ ($\epsilon \ll 1$), which reduces equation (2.2) to : $\epsilon_{XXX} = -\epsilon$. This linear equation admits solutions of the type $\epsilon(X) = \alpha e^{\beta X}$ with $\beta^3 = -1$. Among the tree solutions of this equation, two have positive real parts and thus diverge in the limit $X = +\infty$. We deduce that the only physical solution is $\beta = -1$, which leads to $H = 1 + \alpha e^{-X}$, where α is a constant which reflects the invariance of the dynamical meniscus (2.2) with respect to a translation along X. Close to the film, we thus expect the film thickness to decay exponentially following the law:

$$h(x) = h_0 \left(1 + \alpha.e^{-x/\lambda} \right) \tag{2.3}$$

More generally, equation (2.2) can be integrated numerically down to the meniscus region, starting with the asymptotic shape $H = 1 + \alpha e^{-X}$. Two examples of film profiles obtained from such a numerical integration are displayed in figure 2 for two different values of the constant α. Changing α leads to a translation of the profile. The main observation is that H_{XX} saturates to the value 0.644 in the limit $X = -\infty$ [figure 2-(b)]. This behavior is indeed expected from equation (2.2): at large H, the right hand side of the equation (quickly) vanishes, which means that $d^2 H/dX^2$ (that is, the dimensionless curvature of the profile) tends towards a constant. This property was exploited by Landau and Levich: by matching this constant curvature with the curvature of the top of the static meniscus ($\sqrt{2}\kappa$) allowed them to deduce the thickness of the entrained film:

$$h_0 \approx 0.94 \kappa^{-1} Ca_0^{2/3} \tag{2.4}$$

Using the definition of λ, the characteristic of the dynamic meniscus can then be deduced. It writes:

$$\lambda \approx 0.65 \kappa^{-1} Ca_0^{1/3} \tag{2.5}$$

These laws should be valid provided that the capillary number is much smaller than unity, which ensures that $h_0 \ll \lambda$ (lubrication approximation), $\lambda \ll \kappa^{-1}$ (the dynamic meniscus hardly perturbs the static one), and a negligible role for gravity.

We tested experimentally these different predictions using reflectometry. The experiment consists of illuminating the film with a source of white light and analyzing the interference fringes produced from the light reflected by the film surface and the one reflected by the solid substrate. We use as a substrate a mirror made of silicon. Knowing the indices of both the solid and the liquid, the film thickness can be deduced from the analysis of the interference pattern. The wavelength spectrum is $400 - 800$ nm, and the incident and reflected lights are driven (and collected) using an optical fiber placed at a distance of typically 5 mm from the solid. The thicknesses accessible by this technique range between 20 nm and 30 μm. Less than 1 s is necessary for acquiring a data point,
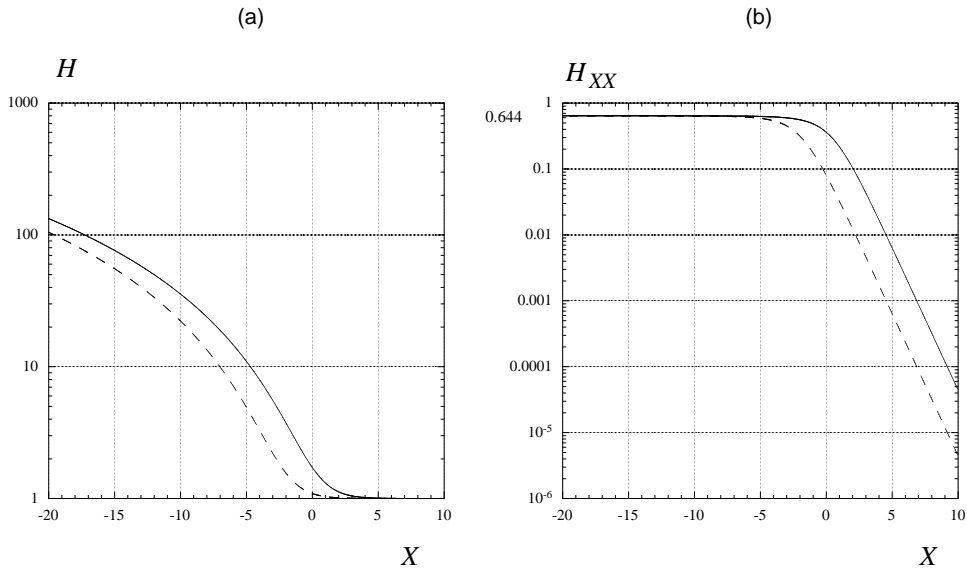
FIGURE 2. (a) Evolution of the film thickness H obtained via the numerical integration of equation (2.2) with the initial profile (2.3) and for two different constant $\alpha = 1$ (solid line) and $\alpha = 0.1$ (dashed line) (b) Evolution of the reduced curvature H_{XX} obtained via the numerical integration of equation (2.2) for two different constant $\alpha = 1$ (solid line) and $\alpha = 0.1$.

and the precision of the measurement is a few nanometers, much smaller than the film thickness (which will rather be in the range of 1 to 10 μm).

We chose silicone oils as liquids. These oils completely wet silicon, and the viscosities we used are 100 mPa s and 350 mPa s(where they are Newtonian, considering the applied shear stresses). The substrate is fixed, and coating is achieved by lowering the reservoir of oil. A step-by-step motor controls the motion of the reservoir, implying coating velocities between 5 μm/s and 25 μm/s, with a precision smaller than 1 μm/s. While the film is deposited, the meniscus moves with respect to the (fixed) optical fiber, which measures the thickness every second, and thus at different points of the dynamic meniscus.

Figure 3-(a) shows an example of such a scan. It was obtained while withdrawing the silicon wafer at a velocity $V = 25$ μm/s out of a silicone oil of surface tension $\gamma = 20$ mN/m and viscosity $\eta = 100$ mPa.s, for which the capillary length κ^{-1} is 1.5 mm. The corresponding capillary number is very low (1.25×10^{-4}) , in the range of applicability of Landau-Levich laws. Then, we expect (from Eq. 2.4) a thickness for the deposited film of 3.5 μm, in excellent agreement with the value observed at large x in figure 3-(a). It is also observed that the film is flat, which confirms that gravity (whose effect is to thin the film) can indeed be neglected in this limit of small capillary numbers. In the same figure, we emphasize that the profile is very well fitted by an exponential function $h(x) = h_0 \left(1 + \alpha e^{-x/L}\right)$, as expected from Eq. 2.3. We deduce from the fit a value for L, which for this particular example is found to be 47 ± 1 μm. This value is in good agreement with the length expected from Eq. 2.5, which is 47 μm.

We repeated this experiment for different oil viscosities and withdrawal velocities, which allowed us to vary the capillary number between 10^{-4} and 2×10^{-4}. In each case, the profile of the dynamic meniscus could nicely be fitted by an exponential law, whose
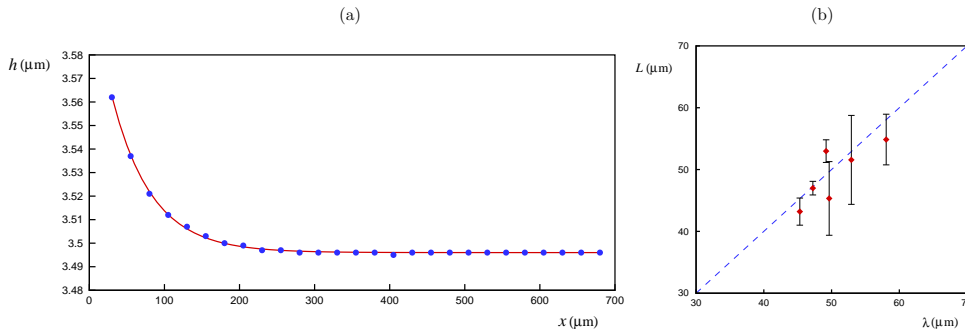
(a)

(b)

FIGURE 3. (a) Stationary profile of the dynamic meniscus in the region of the entrained film, as obtained from a reflectometry experiment, for a silicon wafer drawn at $V = 25\ \mu$m/s out of a bath of silicone oil of surface tension $\gamma = 20$ mN/m and viscosity $\eta = 100$ mPa.s. The dots are the data, and the line is an exponential fit of characteristic length $L = 47\mu$m. (b)Characteristic length L of the dynamic meniscus deduced from fits such as reported in (a) as a function of the length λ expected from Landau-Levich theory and calculated from Eq. (2.5). Both quantities scatter around the line $L = \lambda$.

characteristic length L is plotted in Figure 3-(b) as a function of λ, i.e. the length calculated from Eq. (2.5) for each experiment. There again, the fit is quite good (the data scatter around the line $L = \lambda$), without any adjustable parameter. This first series of experiments thus shows the validity of the description proposed by Landau and Levich, in the limit of small capillary numbers ($Ca < 10^{-3}$).

3. Pushing the wetted plate back into the pool

We now consider what happens as immersing the coated plate inside the bath of the same oil. For each constant immersion velocity V, a stationary profile is observed. There again, the motion distorts the top of the quasi-static meniscus, but the shape of the interface is found to differ considerably from what can be seen as plunging a dry solid at similar velocities in the same bath. As reported in Figure 4, we observe here ripples, instead of a monotonous profile.

The force balance should be the same as earlier, the only difference being that the velocity is now $-V$ instead of V_0. This transformation in Eq. (2.2) yields an equation for the dimensionless profile (where h and x are again scaled by h_0 and λ, given in Eq. (2.4) and (2.5)):

$$\frac{d^3 H}{dX^3} = \frac{H - 1}{H^3} \tag{3.1}$$

Close to the film, the linearisation of equation (3.1) ($H(X) = 1 + \epsilon(X)$) leads to $\epsilon_{XXX} = \epsilon$, whose physical solutions (as noted by Bretherton (1961)) are $\epsilon(X) = \alpha_1^{\beta_1 X}$ and $\epsilon(X) = \alpha_2^{\beta_2 X}$ with $\beta_1 = -1/2 + i\sqrt{3}/2$ and $\beta_2 = -1/2 - i\sqrt{3}/2$. The film thickness thus varies as $H(X) = 1 + \alpha_1 e^{-X/2} e^{i\sqrt{3}/2X} + \alpha_2 e^{-X/2} e^{-i\sqrt{3}/2X}$. Since H is real, we can rewrite the film thickness as:

$$H(X) = 1 + \alpha e^{-\phi/\sqrt{3}} e^{-X/2} \cos\left(\frac{\sqrt{3}X}{2} + \phi\right) \tag{3.2}$$

This function indeed shows an oscillatory behavior, damped by an exponential decay as going to the film region. The phase ϕ reflects the invariance of the dynamical meniscus
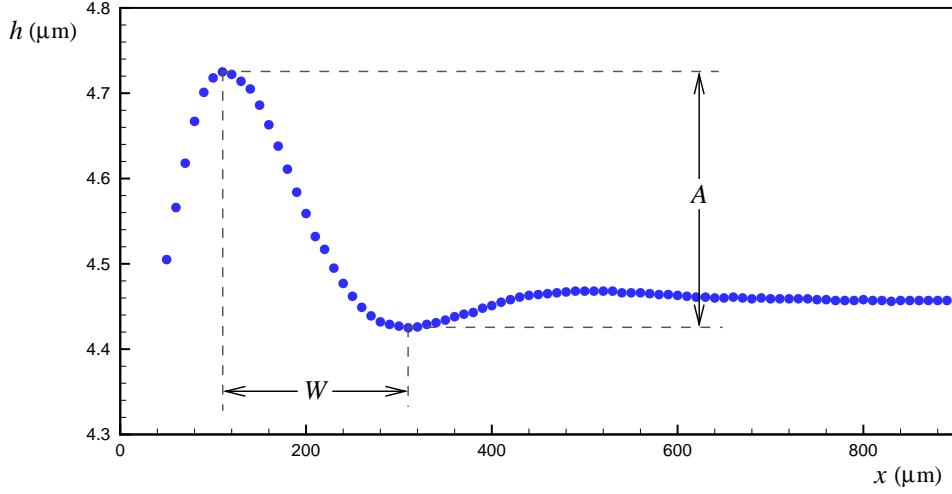
FIGURE 4. Stationary profile of the dynamic meniscus, for a plate coated by a thin film ($h_0 = 4.46$ μm) of silicone oil ($\gamma = 20$ mN/m and $\eta = 350$ mPa.s) immersed at $V = 10$ μm/s inside a bath of the same silicone oil. The data are obtained by reflectometry. The profile is found to be wavy, with a wavelength W of about 200 μm and amplitude A of about 0.3 μm.

(3.1) with respect to a translation along X. The effect of the second constant α can be seen on figure 5.

Examples of film profiles obtained via the numerical integration of equation (3.1) with the initial profile (3.2) are presented on figure 5 for three different values of the constants α and ϕ. Changing ϕ just translates the profile, while changing α affects the amplitude of the oscillations. Apart from the translation, and modification of the oscillations, the main observation is that H_{XX} saturates in the limit $X = -\infty$ [figure 5-(b)]. Unlike the out-going case described by equation (2.2), the reduced curvature saturates to a value which depends on α. The evolution of the saturated curvature $H_{XX}(-\infty)$ is presented on figure 5-(c) as a function of the constant α.

The fact that the reduced curvature does not always reach the same value in the limit $X = -\infty$ should not be a surprise: it is related to the fact that the coating velocity V_0 is independent from the penetration velocity V. This can be shown using the relation $h_{xx} = h_0/\lambda^2 H_{XX}$ from which we get : $H_{XX} = h_0.h_{xx}/(3.Ca)^{2/3}$. Since $h_0 = 0.94$ $\kappa^{-1}Ca_0^{2/3}$ and $h_{xx} = \sqrt{2}$ κ, we find:

$$H_{XX}(-\infty) \approx 0.64 \left(\frac{Ca_0}{Ca}\right)^{2/3} \tag{3.3}$$

If $Ca = Ca_0$ we recover the former limit $H_{XX} = 0.64$. If $V > V_0$ the reduced curvature is lower and the wavy character less pronounced [figure 5]. On the other hand ($V < V_0$), H_{XX} is larger and the profile more wavy. According to equation (3.3) the ratio V_0/V, which is controlled experimentally, imposes the reduced curvature H_{XX}. One can thus find a corresponding value for the constant α [figure 5-(c)] and compare the experimental profile to the theoretical one.

Considering the experiments, equation (3.1) also suggests that the results should rather be presented in this dimensionless fashion, which is done in Figure 6 for two different experiments. It is observed that the data collapse in a unique curve. This curve is fairly well fitted by the numerical solution of Eq. (3.1) (drawn in full line), which is solved and matched with the film (which yields a solution very close to Eq. (3.2) with $\alpha = 1$). The
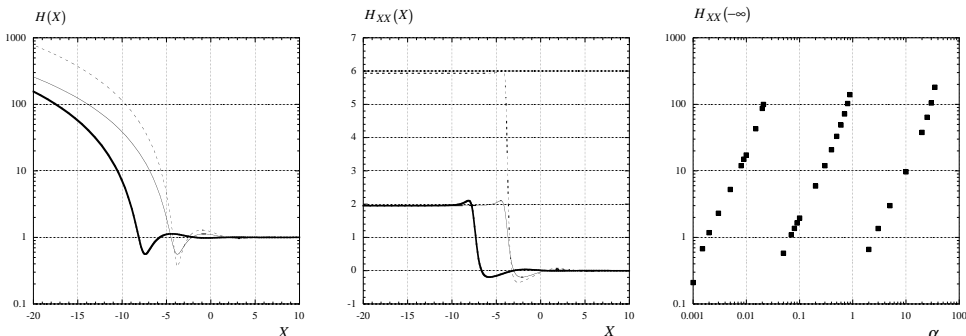
FIGURE 5. (a) Evolution of the film thickness H obtained via the numerical integration of equation (3.1) with the initial profile (3.2) and for different constants $\alpha = 0.1$, $\phi = 0$ (thin solid line), $\alpha = 0.1$, $\phi = \pi$ (thick solid line) and $\alpha = 0.2$, $\phi = 0$ (thin dashed line). (b) Evolution of the reduced curvature H_{XX} obtained via the numerical integration of equation (3.1) for different constants $\alpha = 0.1$, $\phi = 0$ (thin solid line), $\alpha = 0.1$, $\phi = \pi$ (thick solid line) and $\alpha = 0.2$, $\phi = 0$ (thin dashed line). (c) Evolution of the constant curvature $H_{XX}(-\infty)$ as a function of the constant α.

fit nicely captures the period of the wave, yet slightly overestimates the height of the largest bump. This numerical solution also predicts the existence of a second minimum close to $X = 0$, but this region could not be characterized experimentally, owing to the very large slope of the profile at small X, which makes it impossible to get reflectometry data.

4. Wave versus wedge.

The shape of meniscus could have been very different: as noted above, when forcing a (dry) plate to enter a bath the deformation is very different in shape: a liquid wedge forms at the top of the meniscus, forming there a dynamic angle θ which is known to be fixed by the value of the corresponding capillary number. For a wetting liquid, this angle obeys the so-called Tanner's law (Tanner (1979)), which specifies that the angle increases as the cubic root of the capillary number, for small Ca ($Ca \ll 1$):

$$\theta = \zeta Ca^{1/3} \tag{4.1}$$

where ζ is a numerical constant, which was found experimentally to be of the order of 4.5.

Eq. (4.1) can be understood as follows [de Gennes (1985)]. Surface tension resists deformation, and generates a restoring force which can be written $\gamma(1 - \cos\theta)$, per unit length of the contact line. In the limit of small angles, this force reduces to $\gamma\theta^2/2$. The viscous force responsible for the deformation can be calculated by integrating the quantity $\eta\nabla u$ within the wedge. This quantity scales as $\eta V/\theta x$ (where the origin of x is taken at the top of the wedge), which must be integrated over x. Hence a logarithmic divergence, which can be treated by introducing a cut-off a at small x, corresponding physically to a (microscopic) slip, or to the presence of a (microscopic) wetting film. We note Γ this logarithmic term. Γ is of the order of 15 for a dry solid [$\Gamma \approx \ln(\kappa^{-1}/a)$], and can be significantly smaller, of order 6, if the wedge slips on a film of thickness h_0
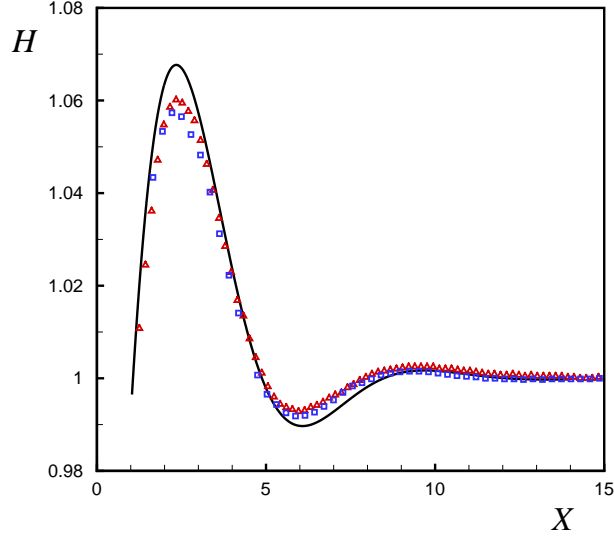
FIGURE 6. Stationary profile of the dynamic meniscus, for a plate coated by a thin film at a velocity V with a film of silicone oil ($\gamma = 20$ mN/m and $\eta = 350$ mPa.s) and then immersed at V inside a bath of the same oil. The film thickness is scaled by the thickness of the deposited film, and the x coordinate by the Landau-Levich length of dynamic meniscus [Eq. (2.5)]. The data correspond to $V = 10$ μm/s (triangles) and to $V = 20$ μm/s (squares). The line is the numerical solution of Eq. (3.1), with a matching condition with the film (which yields a solution very close to Eq. (3.2), with $\alpha = 1$)

of a few micrometers ($\Gamma \approx \ln\left(\kappa^{-1}/h_0\right)$. The viscous force is thus found to scale as $\eta V/\theta$, with a numerical coefficient which includes Γ. Balancing this force with the capillary force $\gamma\theta^2/2$ yields Tanner's law [Eq. (4.1)].

We can thus calculate the rate of energy dissipation $\dot{E}$ in both the wedge geometry, and for the wavy profile. In each case, we know the velocity profile and the geometry of the flow, so that we can calculate this rate, expressed as $\eta \int \left(\nabla u\right)^2 d\Omega$, where the integral is calculated on the volume Ω of the liquid corner. For the wedge geometry, we find:

$$\dot{E} \approx 1.65 \, \Gamma^{2/3} \, \gamma V C a^{2/3} \tag{4.2}$$

For the wavy profile, there is a film which is first deposited, whose thickness obeys Eq. (2.4): $h_0 = 0.94\kappa^{-1}Ca_0^{2/3}$, where we denoted Ca_0 as the capillary number at which the deposition was achieved (in a general case, the deposition velocity can differ from the immersion velocity). Knowing the interface profile in this case [Eq. (3.2)], we can also calculate the rate of energy dissipated by viscosity. It writes:

$$\dot{E} \approx 1.34 \, \gamma V C a_0^{2/3} \left(\frac{V_0}{V}\right)^{2/3} \tag{4.3}$$

In the particular case when deposition and immersion are performed at the same speed ($Ca = Ca_0$), the latter expression reduces to:

$$\dot{E} \approx 1.34 \, \gamma V C a^{2/3} \tag{4.4}$$

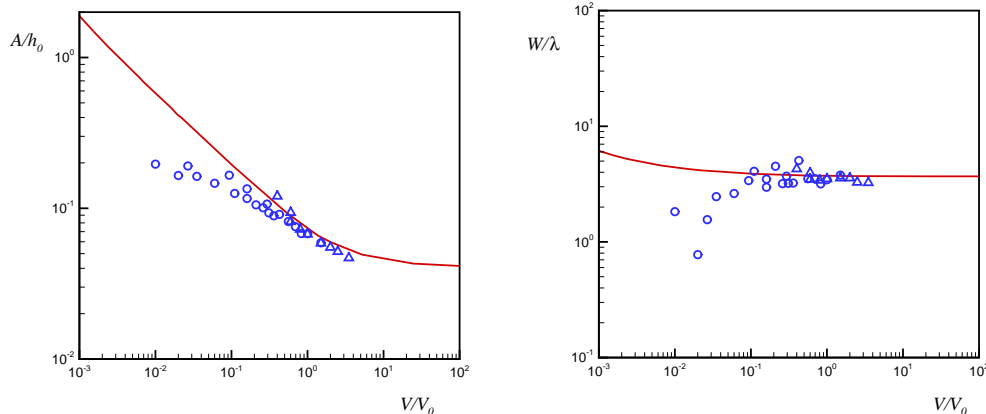whose scaling is similar to the one in the wedge [Eq. (4.2)]. In this case ($V = V_0$), and

FIGURE 7. Dimensionless amplitude and wavelength of the wavy pattern as a function of the ratio between the withdrawal and immersion velocities. Circles: experimental data for silicone oil with viscosity 100 mPa. s, and triangles: viscosity 350 mPa.s. Solid line: numerical data.

taking $\Gamma = 6$, we find that the coefficient in Eqs. (4.2) and (4.4) are about 10 and 1.34, respectively, which shows that the energy dissipated by viscosity is significantly smaller in the wavy meniscus than in the wedge. This might explain why in this case we always observe a wavy meniscus (as reported in Figs. 4 and 6), which in addition is nicely fitted by the expected profile [Eq. (3.2) and Fig. 6].

In a more general case, we must compare Eqs. (4.2) and (4.3), and the dissipation is minimal in the wavy meniscus provided that:

$$\frac{V}{V_0} > \frac{1}{1.37\,\Gamma} \approx 0.1 \tag{4.5}$$

In order to check this criterion, we did a series of experiments where we varied in a large extent the velocities V_0 and V of both the withdrawal (which fixes the thickness of the deposited film) and the immersion. In each case we measured the amplitude A of the maximum peak, in the wavy part, and the wavelength W of the interface presented on figure 4. For each experiment, we calculated the expected profile [Eq. (3.2)], and deduced from these calculations the theoretical values of A and W. We report in Figure 7 the comparison between both quantities (scaled by h_0 and λ, respectively), as a function of the ratio V/V_0, which appears to be the quantity to consider, as seen from Eq. (4.5).

The agreement between the measured and calculated amplitude and wavelength of the oscillation of the profile is quite good, provided that the ratio V/V_0 is large enough. Below a value of the order of 0.1, which is the same in both graphs, the data deviate more and more from the theoretical values, as expected from equation (4.5). This transition remains to be described and understood.

5. Conclusion

We studied by reflectometry the characteristics of the dynamic meniscus, that is the transition region between a static meniscus and a film deposited on a moving solid. If the solid is extracted from the bath, the shape of the "stretched" dynamic meniscus was found to be exponential (close to the deposited film), with a characteristic length slowly increasing as a function of the capillary number (as $Ca^{1/3}$). These features are in excellent agreement with the classical Landau-Levich picture.

Once coated with a film, the plate can be immersed in the bath. Looking at the simple case where both the deposition and the coating velocities are of the same order, it was observed that the dynamic meniscus presents a wavy shape. We studied the amplitude, wavelength and envelope of this shape, and found that all these characteristics are very well understood by taking into account an old remark made by Bretherton.

It is worth wondering why such a shape shows up, instead of the classical wedge observed when plunging a dry solid in a wetting bath. By comparing the viscous dissipation in both cases (i.e. wave versus wedge), we showed that the wavy shape corresponds to a minimum dissipation, provided that the immersion velocity is larger than about 10% of the deposition velocity. If this criterion is not obeyed, our experiments indicate that the Bretherton picture does indeed not capture anymore the meniscus profile, implying a transition towards a less well-defined shape. We plan in the future to describe this regime, in order to understand if (and how) the system then moves towards a wedge, the solution classically observed in the case of a zero deposition velocity (i.e. dry solid). In the latter case, our calculations indeed show that the dissipation in a wedge is smaller than in a wavy meniscus, making it clear why the first of these shapes is then observed.

REFERENCES

F.P. BRETHERTON 1961 The motion of long bubbles in tubes In *Journal of Fluid Mechanics* **10** pp. 166.

DERJAGUIN B. 1943 Thickness of liquid layer adhering to walls of vessels on their emptying and the theory of photo- and motion picture film coating In *Comptes Rendus (Doklady) de l'Academie des Sciences de l'URSS* **XXXIX** pp. 13-16.

EGGERS J. 2004 Towards a description of contact line motion at higher capillary numbers In *Phys. Fluids* **16** pp. 3491-3494.

P.G. DE GENNES 1985 Wetting: statics and dynamics. *Rev. Mod. Phys.* **57** pp. 827–863.

HOFFMAN, R.L. 1975 A study of the advancing interface: I. Interface shape in liquid-gas systems *J. Colloid Interface Sci.* **50** pp. 228-241.

LANDAU L. AND LEVICH B. 1942 Dragging of a liquid by a moving plate In *Acta Physicochimica U.R.S.S.* **17** pp. 42-54.

J.C. MAXWELL 1875 Capillary Action. *Encyclopaedia Britanica* **9**th **ed.**

PARK, C.W. AND HOMSY, G.M. 1984 Two-phase displacement in Hele Shaw cells: theory In *Journal of Fluid Mechanics* **139** pp. 291-308.

QUÉRÉ D. 1999 Fluid coating on a fiber In *Ann. Rev. Fluid Mech.* **31** pp. 347-384.

RUSCHAK K.J. 1985 Coating flows In *Ann. Rev. Fluid Mech.* **17** pp. 65-89.

L. TANNER 1979 The spreading of silicone oil drops on horizontal surfaces. *J. Phys. D: Appl. Phys.* **12** pp. 1473–1484.